Journal of Current Science and Technology, May-August 2021 JCST Vol. 11 No.2, pp. 299-310

ISSN 2630-0656 (Online)

Cite this article: Thungsatianpun, N., Mavichak, R., T-Thienprasert, N., Unajak, S.,& Sinthuvanich, C. (2021, May). Cell-penetrating peptide nanocomplexes enhanced cellular uptake of dsRNA in Sf9 cell line. *Journal of Current Science and Technology, 11*(2), 299-310. DOI:10.14456/jcst.2021.30

Journal of Current Science and Technology

Journal homepage: https://jcst.rsu.ac.th

Cell-penetrating peptide nanocomplexes enhanced cellular uptake of dsRNA in Sf9 cell line

Narita Thungsatianpun[1], Rapeepat Mavichak[2], Nattanan T-Thienprasert[1], Sasimanas Unajak[1], and Chomdao Sinthuvanich*[1, 3]

[1]Department of Biochemistry, Faculty of Science, Kasetsart University, Bangkok 10900, Thailand
[2]Aquatic Animal Health Research Center, Charoen Pokphand Foods Public Company Limited, Samutsakorn 74000, Thailand
[3]Specialized center of Rubber and Polymer Materials in agriculture and industry (RPM), Faculty of Science, Kasetsart University, Bangkok 10900, Thailand

*Corresponding author; E-mail: chomdao.si@ku.th

Received 28 March 2021; Revised 30 April 2021; Accepted 5 May 2021;
Published online 27 May 2021

Abstract

The use of double-stranded RNA (dsRNA) to knock down genes of interest has gained increased attention in arthropods for applications in insect pest management and vaccine development for aquatic animals. However, its large size and highly anionic character impede the internalization of dsRNA into cells. To improve cellular uptake, we utilized cell-penetrating peptides (CPPs) as a delivery vehicle to carry dsRNA across the cell membrane. Here, nanocomplexes prepared from 600-bp dsRNA and CPPs, TAT or EB1, were characterized and their ability to carry dsRNA into cells was investigated. The optimal positive to negative charge (P/N) ratio between CPPs and dsRNA was determined by electrophoresis mobility shift assay and fluorescence spectroscopy. Hydrodynamic size and zeta potential of the complexes were assessed by the dynamic light scattering technique. Morphology and size distribution of nanocomplexes were examined by transmission electron microscope. Cellular uptake of CPP/dsRNA nanocomplexes was evaluated in *Spodopteria frugiperda* (Sf9) cell line. Internalized dsRNA levels were assessed by semi-quantitative reverse transcription (RT)-PCR after 1, 6, and 48 h. The results showed that at an appropriate charge ratio, cationic complexes can be formed with size in the range of nanometers. Interestingly, regardless of CPPs used, the 600-bp dsRNA were internalized into the cell during the first hour of incubation. However, levels of dsRNA delivered by TAT were diminished, comparing to EB1 after 48 h. Overall, this work provides more insights into the factors involving nucleic acid delivery in arthropod cells.

Keywords**:** *cell-penetrating peptide; cellular uptake; double-stranded RNA; nanocomplex; Spodopteria frugiperd.*

1. Introduction

RNAi is a naturally occurring post-transcriptional gene silencing process that regulates mRNA expression level in the cells. RNAi is triggered by cleavage of long double-stranded RNA (dsRNA) by Dicer, an RNase III endoribonuclease, into short nucleotide fragments or small interfering RNA (siRNA). This double-stranded siRNA is unwound, and the resulting single-stranded RNA is loaded onto the RNA-induced silencing complex (RISC). The complex bind to the target mRNA leading to mRNA degradation. RNAi is a versatile research tool to study cellular functions and pathways by the introduction of exogenous dsRNA into cells to induce gene-specific knockdown (Sifuentes-Romero, Milton, & García-Gasca, 2011). In agricultural applications, dsRNA has been proposed as a promising candidate for biocontrol of insect pest (Christiaens, Niu, & Taning, 2020; Cooper et al., 2021; Edwards et al., 2020; Lin, Huang, Liu, Belles, & Lee, 2017), management of pollinators (Brutscher & Flenniken,

2015), and protection of aquatic animals from viral diseases (Attasart et al., 2009; Sanitt et al., 2016; Theerawanitchpan et al., 2012; Ufaz et al., 2018). RNAi is considered as a powerful strategy alternative to the introduction of synthetic chemicals due to the low toxicity, high specificity, and environmental-friendly of exogenous dsRNA molecules. Moreover, dsRNA can be produced *in vitro* by an RNase III-deficient *E. coli* strain allowing for large-scale production that is economically feasible for industrial use.

Sf9 cell line is derived from *Spodoptera frugiperda* Sf21 cells. In addition to commonly being used for protein expression by the baculovirus system, the Sf9 cell line has been used as a model cell for dsRNA development for application involving RNAi in arthropods. For example, nanoparticles derived from cationic polymers were studied in the Sf9 cells as a representative lepidopteran cell line (Laisney, Gurusamy, Baddar, Palli, & Unrine, 2020). The chitosan-based delivery system of dsRNA was developed and tested on the Sf9 cells for the protection of the shrimp virus (Theerawanitchpan et al., 2012). However, the RNAi efficiency is varied from species to species which are results of several possibilities such as different RNAi pathways (Joga, Zotti, Smagghe, & Christiaens, 2016), stability of exogeneous RNA (Shukla et al., 2016), and available transmembrane protein i.e. SID-1 and SID-2 on the cell surface (Feinberg & Hunter, 2003; McEwan, Weisman, & Hunter, 2012).

One particular problem that may limit the use of dsRNA in agriculture applications is its low cellular uptake efficiency. Intrinsic properties of dsRNA such as relatively large size and highly negative charge possess as a barrier for efficient RNAi in the cells. To improve cellular uptake, several approaches were applied such as the incorporation of cationic polymer (Dhandapani, Gurusamy, Howell, & Palli, 2019; Gurusamy, Mogilicherla, & Palli, 2020; Kim, Kim, Akaike, & Cho, 2005; Theerawanitchpa et al., 2012), the combination with dendrimer-coated carbon nanotube (Edwards et al., 2020), and the encapsulation in liposomes (Lin et al., 2017; Sanitt et al., 2016). In addition to those, cell-penetrating peptides (CPPs), a family of short peptides capable of translocation across the cellular membrane, are promising carriers for dsRNA delivery.

CPPs have been proven useful as a powerful research tool to deliver various cargoes into cytoplasm including drugs (Xie et al., 2020), nanoparticles (Uhl et al., 2020), liposomes (Liu et al., 2017), and biomolecules (Cermenati et al., 2011). A classic example of CPPs is TAT, an arginine-rich 11-amino-acid peptide, derived from a trans-activator protein of human immunodeficiency virus (HIV)-1 (Green & Loewenstein, 1988; Frankel & Pabo, 1988). Complexation between TAT and nucleic acids allows translocation of small interfering RNA (siRNA) and plasmid DNA across plasma membrane primarily via endocytosis (Al Soraj et al., 2012). Nevertheless, nucleic acid delivery mediated by several CPPs, including TAT, encounters an issue with endosomal entrapment preventing the release of cargoes from the endosome into the cytoplasm where RNAi process occurs (Kaplan, Wadia, & Dowdy, 2005). To overcome this problem, endosomolytic CPPs have been developed such as EB1, a 23-amino acid peptide that incorporates histidine and tryptophan residues into the sequence. This allows the cargoes to escape out of the endosome and are released into the cytoplasm (Lundberg, El-Andaloussi, Sütlü, Johansson, & Langel, 2007). Regardless of delivery mechanism, delivery of nucleic acids, such as siRNA and plasmid DNA, by non-covalent complexation with CPPs has been extensively studied particularly in mammalian cells (Cerrato et al., 2020; Huang, Lee, Tolliver, & Aronstam, 2015; Liu, Huang, Aronstam, & Lee, 2016). However, only a few studies have investigated the delivery of long dsRNA using CPPs (Wei et al., 2015). In this study, we explored the possibility of using CPPs, particularly TAT and EB1, as a carrier to improve cellular uptake of long dsRNA in the arthropod cell line, Sf9 cells.

2. Objectives

This research aimed to explore the possibility of using CPPs as a carrier to improve cellular uptake of long dsRNA in the arthropod Sf9 cell line. The ratios between CPPs and dsRNA for nanocomplex formation were optimized. The physical properties and morphology of CPPs/dsRNA nano complexes were characterized and the cellular uptake efficiency of dsRNA was compared between the two CPPs.

3. Materials and methods

3.1 Cell-penetrating peptides

Two CPPs with >95% purity were purchased from Cellmano Biotech Limited (Hefei,

China). Peptides were synthesized by solid-phase peptide synthesis with Fmoc chemistry. The carboxyl terminus of peptides was amidated. Lyophilized peptides were dissolved in ultrapure nuclease-free water, aliquoted, and stored at -20 °C.

3.2 Preparation of dsRNA

A plasmid DNA (pET-17b) encoding for dsRNA targeting viral mRNA of ribonucleotide reductase small subunit (*rr*2) was transformed into an RNase III-deficient *E. coli* strain HT115. The plasmid containing the *rr*2 gene was obtained from Dr. Rapeepat Mavichak. For dsRNA production, the cells were cultured in 2x YT medium supplemented with 0.1 mg/ml ampicillin and 0.0125 mg/ml tetracycline at 37 °C for 3 h at 220 rpm until O.D. at 600 nm reached 0.4. After that, 1 mM isopropyl β-D-1-thiogalactopyranoside was added and the cells were further incubated at 37 °C for 3 h until O.D. at 600 nm was 1.0. RNA was extracted according to the protocols adapted from Attasart et al. (2009). Briefly, the cell pellet was collected by centrifugation and resuspended in 0.1% (w/v) sodium dodecyl sulfate (SDS) followed by boiling at 100 °C for 2 min. To eliminate single-stranded RNA, 1 μg of RNase A was added per 100 μl of reaction in 50 mM Tris-HCl pH 8.0 and incubated at 37 °C for 5 min. After that, the dsRNA was extracted using TRI reagent (Molecular research center, Inc., Cincinnati, Ohio, USA) according to the manufacturer's instruction. The quality of extracted dsRNA was evaluated by a Nanodrop spectrophotometer (Thermo Fisher Scientific, Waltham, Massachusetts USA) and agarose gel electrophoresis.

3.3 Electrophoretic mobility shift assay

CPPs and dsRNA were separately dissolved in ultrapure nuclease-free water. Then, one μg of dsRNA solution was mixed with CPPs solution at different P/N ratios, where P is the number of positive charges on CPPs and N is the number of negative charges on dsRNA. The mixture was incubated at room temperature for 30 min. The mobility of the complexes was monitored by 1% (w/v) agarose gel electrophoresis in a tris-borate-EDTA (TBE) running buffer at 100 volts for 40 min. The gel was stained with GelRed® Nucleic Acid Gel Stain (Biotium Inc., Fremont, California, USA). The number of charges was calculated from the following equations:

Negative charges on dsRNA = mol of dsRNA x 600 nucleotides

Positive charges on TAT = mol of peptide x 9

Positive charges on EB1 = mol of peptide x 10

3.4 Quantitative fluorescence intensity

CPP/dsRNA complexes were prepared by mixing CPP with dsRNA solution at various P/N ratios in a black 96-well plate. After 30 min of incubation at room temperature, 0.1 ml of QuantiFluor® RNA Dye (Promega Corporation, Madison, Wisconsin, USA) was added into each well. The fluorescence intensity was measured at the excitation wavelength of 485 nm and emission wavelength of 535 nm using a fluorescence microplate reader (Infinite200 PRO, Tecan Group Ltd., Switzerland). The binding efficiency of CPP/dsRNA was calculated as percent of free dsRNA. Standard deviation was calculated from three replicates. The percent of free dsRNA was calculated from the following equation:

% free dsRNA = fluorescence intensity of complexes/fluorescence intensity of naked dsRNA) x 100

3.5 Determination of zeta potential, size, and morphology of CPP/dsRNA

To determine the hydrodynamic size and zeta potential, each CPP was mixed with dsRNA at various P/N ratios. Briefly, the peptide solution was mixed with 1 μg of dsRNA to a final volume of 0.1 ml in nuclease-free water. The mixture was agitated by pipetting and vortexing for 30 sec followed by incubation at room temperature for 30 min. After that, CPP/dsRNA complex was brought up to 1.0 ml in ultrapure nuclease-free water. Hydrodynamic size and zeta potential of the complexes were measured using a Zetasizer Nano (ZEN3600, Malvern Panalytical Ltd, UK). All measurements were performed in quintuplicate at room temperature. Statistical analysis was assessed by one-way ANOVA with Tukey's post hoc comparison using jamovi 1.6.13 software.

To visualize the morphology of the nanocomplexes, transmission electron microscopy was performed at a 50:1 P/N ratio. After preparing the solution as previously described, the diluted solution was dropped onto a 300-mesh copper grid and allowed to dry for 30 min. Then, the mixture was stained with 2% uranyl acetate for 30 sec and

analyzed using a transmission electron microscope (HT-7700, Hitachi, Japan) at 120 kV at the Scientific Equipment and Research Division, Kasetsart University Research and Development Institute.

3.6 Semi-quantitative PCR analysis of dsRNA internalization

Sf9 (*Spodoptera frugiperda*) cells were seeded onto a 24-well plate at a density of 1.5×10^5 cells/0.5 ml/well in serum-free Sf-900™ III SFM media (Thermo Fisher Scientific, Waltham, Massachusetts, USA) supplemented with 1% (v/v) penicillin-streptomycin. After incubation at 27 ºC overnight, CPP/dsRNA complexes at P/N ratio of 1:1 and 50:1 were added to the cells. Cells treated with 1 µg dsRNA were used as a control. After 1, 6, and 48 h of incubation, cells were washed three times with phosphate buffer saline (PBS) (pH 7.4) to remove uninternalized dsRNA. Then, 0.2 ml of TRI reagent (Molecular research center, Inc., Cincinnati, Ohio, USA) was added into each well, and cells were homogenized using a syringe equipped with a 23-gauge needle. Cell lysates from three wells were pooled and total RNA was isolated according to the manufacturer's protocol. After that, DNA was removed by treatment with DNase I (Thermo Fisher Scientific, Waltham, Massachusetts, USA). The quality of extracted RNA was analyzed by a Nanodrop spectrophotometer (Thermo Fisher Scientific, Waltham, Massachusetts USA). Then, 2 µg of RNA was synthesized to the first-strand cDNA with Viva 2-step RT- PCR Kit with M-MuLV/Taq DNA polymerase (Vivantis Technologies Sdn. Bhd., Selangor, Malaysia).

The internalized dsRNA was amplified by PCR with the following primer: *rr*2-Fw (5'-AGG GAC GAA GGT CTT CAT CG-3') and *rr*2-Rv (5'-GAG GAG GTG CAG TCA GAA TT-3') (Liu, Chang, Wang, Kou, & Lo, 2005). EF-1α gene of *Spodoptera frugiperda* was used as a reference gene. The sequences of EF-1α primers were as followed: EF-1α -Fw (5′-TGG GCG TCA ACA AAA TGG A 3′) and EF-1α -Rv (5′-TCT CCG TGC CAG CCA GAA AT -3′) (Shu, Zhang, Zeng, Cui, & Zhong, 2019). The PCR cycle was as followed: 94°C for 2 min; 20 cycles of 94°C for 30 s, 54.5 ºC for *rr*2 and 54.2 ºC for *EF-1α* for 30 s, 72°C for 30 s; followed by a final extension at 72°C for 7 min. Each PCR product was analyzed by 1% agarose gel electrophoresis. The intensity of *EF-1α* and *rr*2 bands was quantified using Image J (Schneider, Rasband, & Eliceiri, 2012). Statistical analysis was assessed by one-way ANOVA with Tukey's post hoc comparison using jamovi 1.6.13 software. The internalization experiments were performed independently in triplicate.

4. Results and Discussion

4.1 Complexation between dsRNA and CPPs

The formation of nanocomplexes between CPPs and dsRNA relies on electrostatic interaction. At the optimal charge ratio between cationic functional groups of peptides, such as amine and guanidinium, and the phosphate group of RNA, cationic nanocomplexes can be readily produced. This cationic character and the small size facilitate cellular uptake of dsRNA (Foroozandeh & Aziz, 2018). Two CPPs, TAT and EB1, with similar charge but distinct mechanism of endosomal release, were used in this study to investigate the physical character and cellular uptake efficiency of the nanocomplexes. The sequences and charge of CPPs are shown in Table 1.

Table 1 Cell-penetrating peptide used in this study

Name	Sequence	Charge
TAT	YGRKKRRQRRR-NH_2	+9
EB1	LIRLWSHLIHIWFQNRRLKWKKK-NH_2	+10

To determine the optimal charge ratio, a fixed concentration of dsRNA was mixed with CPP solution at an increased positive/negative (P/N) charge ratio. Here, negative charges of dsRNA were neutralized by positive charges of peptides resulting in retardation of dsRNA mobility as observed by gel electrophoresis. As shown in Figure 1A, at the P/N ratio of 0.1:1, TAT binds to dsRNA as indicated by a shift of dsRNA band to a higher molecular weight. Increasing the amount of TAT, the migration of dsRNA was completely retarded. A similar trend was observed for EB1 of which dsRNA bands were shifted at a P/N ratio of 0.1:1 and 1:1, and disappeared at P/N ratio greater than 2:1.

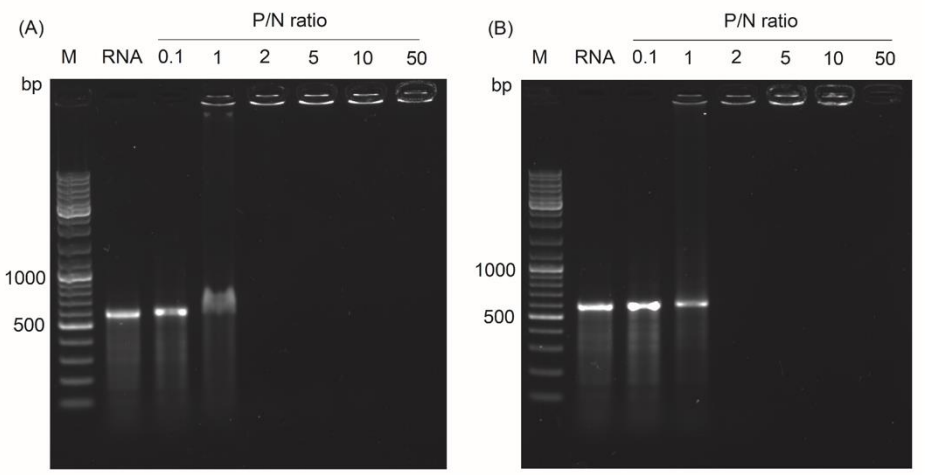

Figure 1 Electrophoretic mobility shift assay of CPP/dsRNA complexes prepared at different P/N ratios with 0.1 µg of dsRNA. Lane M: 100-bp DNA marker. Lane RNA: naked dsRNA. (A) TAT/dsRNA complex. (B) EB1/dsRNA complex.

The ability of CPPs to form a complex with dsRNA was further quantified using QuantiFluor® RNA Dye. Here, the fluorescent RNA-binding dye bind to free dsRNA molecules that were not incorporated into the CPP/dsRNA complex. Thus, with the increasing amount of CPPs, the fluorescence quenching indicated complex formation. As shown in Figure 2, TAT was able to bind to dsRNA with the optimal P/N ratio lower than 2:1. EB1 required a slightly higher ratio to fully condense the dsRNA. This quantitative experiment confirmed the results of electrophoretic mobility shift assay suggesting that 600-bp dsRNA can complex with short CPPs.

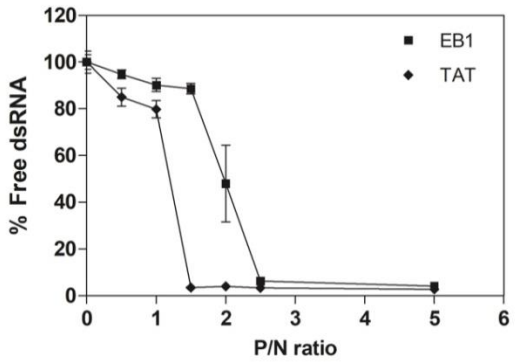

Figure 2 CPP/dsRNA complex formation assessed by QuantiFluor® RNA Dye. The dsRNA solution was incubated with CPPs from 0.5:1 to 5:1 P/N ratios for 30 min. The free dsRNA was normalized to that of naked dsRNA. The error bars were calculated from three replicates

4.2 Characterization of CPP/dsRNA complex

To characterize the physical character of CPP/dsRNA nanocomplexes, the hydrodynamic size and net charge were evaluated by the dynamic light scattering (DLS) technique. Here, 1 µg of dsRNA was mixed with various amounts of CPPs at a P/N ratio ranging from 0.1 to 50. The results showed that the PDI value and zeta potentials of nanocomplexes prepared from TAT and EB1 at the same P/N ratio were not significant difference ($p < 0.01$). As shown in Table 2, the hydrodynamic size of TAT/dsRNA complexes at the P/N ratio of 0.1:1 was 403 ± 328 nm with polydispersity index (PDI) value close to 1.0 implying a broad range of size distribution. Upon increasing P/N ratio, the complexes were condensed to 233 ± 30 nm at 50:1 P/N ratio with a narrow PDI (< 0.3), indicating homogeneous size distribution. A similar trend was observed in EB1/dsRNA nanocomplexes where the P/N ratio increased, the particle size decreased. The zeta potential of EB1/dsRNA nanocomplexes also followed the same trend where the zeta potential was negative at a P/N ratio lower than 2:1. As expected, upon increasing the amount of CPPs to P/N ratio of 50:1, zeta potential increased to +22.9 ± 1.3 mV and +25.7 ± 2.0 mV for TAT/dsRNA and EB1/dsRNA nanocomplexes, respectively. From DLS data, the nanocomplexes prepared at a 50:1 P/N ratio were selected for further investigation due to their small diameters, low PDI values and zeta potential that were closer to 30 mV (Clogston & Patri, 2011; Foroozandeh & Aziz, 2018).

Table 2 Size and zeta potential of nanocomplexes preparing using different CPPs. Data are presented as mean ± S.D. (n = 5)

CPPs	P/N Ratio	Diameter (nm) ± S. D.	PDI ± S. D.	Zeta potential (mV) ± S. D.
TAT	0.1:1	403 ± 328	0.87 ± 0.17	-1.4 ± 1.4
	1:1	285 ± 44	0.35 ± 0.07	-24.3 ± 2.9
	2:1	244 ± 52	0.23 ± 0.08	8.5 ± 1.1
	5:1	209 ± 47	0.28 ± 0.05	15.7 ± 1.6
	10:1	179 ± 27	0.32 ± 0.10	18.1 ± 4.8
	50:1	233 ± 30	0.29 ± 0.03	22.9 ± 1.3
EB1	0.1:1	177 ± 167	0.58 ± 0.35	-6.2 ± 5.8
	1:1	561 ± 559	0.58 ± 0.13	-17.1 ± 3.9
	2:1	251 ± 100	0.42 ± 0.07	7.5 ± 3.7
	5:1	218 ± 46	0.47 ± 0.12	17.5 ± 1.2
	10:1	192 ± 16	0.41 ± 0.04	19.8 ± 1.0
	50:1	216 ± 42	0.36 ± 0.05	25.7 ± 2.0

To visualize and further assess the size of the nanocomplexes, transmission electron microscopy (TEM) was performed on the complexes at a 50:1 P/N ratio. The morphology of TAT/dsRNA nanocomplexes appeared in a spherical shape (Figure 3A and S1). The average size was 29 ± 15 nm under TEM analysis (n = 12), Figure 3B. The morphology of EB1/dsRNA nanocomplexes was also in a spherical shape (Figure 3C and S2) and the average size was 17 ± 6 nm under TEM analysis (n = 73), Figure 3D. The size of the nanocomplexes obtained from TEM analysis was smaller than that from the DLS technique. This is because in TEM experiments, the samples were prepared in the dry format while in DLS, samples were prepared in solution. In this study, 600-bp dsRNA carries a net negative charge from the phosphate group while CPPs with a molecular weight ranging from 1.6 - 3.1 kDa contain a net positive charge. Upon binding, the negative charges of dsRNA were neutralized by positive charges of the peptides. As a result, dsRNA was condensed to form complexes that were reduced in size. With sufficient amounts of peptide, the stable cationic nanocomplexes were obtained.

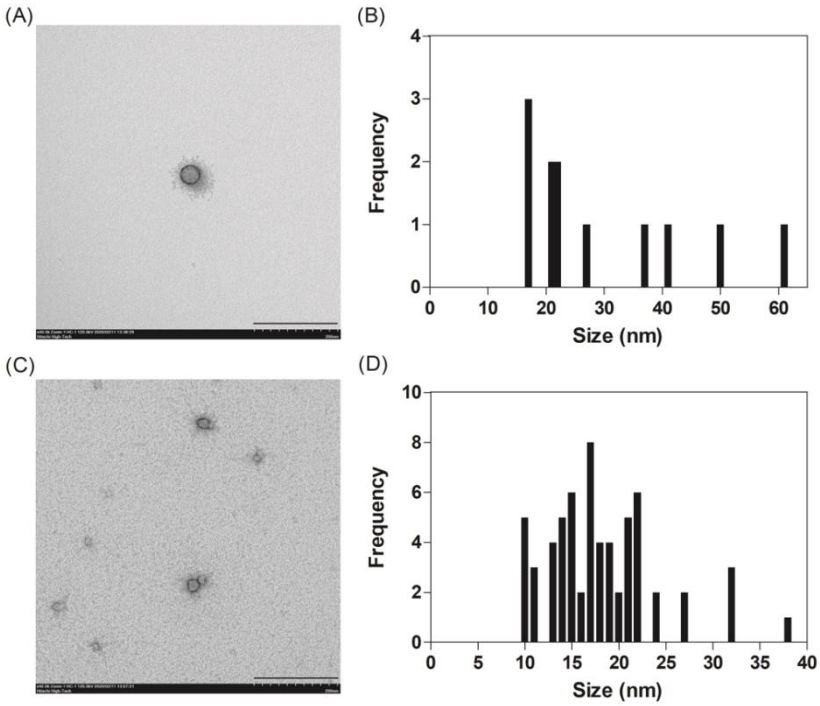

Figure 3 Representative TEM micrographs of CPP/dsRNA nanocomplexes at P/N ratio of 50:1; (A) TAT, (C) EB1; Scale bar = 200 nm. Frequency distribution of measured diameter; (B) TAT, n=12, (D) EB1, n=73.

4.3 Cellular uptake of CPP/dsRNA nanocomplexes

For purpose of studying cellular uptake, we use dsRNA available in the laboratory that targets *rr*2 mRNA of white spot syndrome virus, a shrimp's pathogen. The lack of viral mRNA target in Sf9 cells allows for detection of internalized dsRNA levels without interference from RNAi-mediated dsRNA degradation that typically observed within 24-72 h. To evaluate the efficiency of dsRNA delivery, Sf9 cells were incubated with CPP/dsRNA nanocomplexes prepared at 1:1 and 50:1 P/N ratio. The cells were collected at 1 and 6 h to monitor the initial uptake of dsRNA. In addition, to ensure that dsRNA that survive the endosomal entrapment was observed, the cells were also collected at 48 h. After incubation at a given period, dsRNA molecules that were not internalized into the cells were removed by repetitive washing. Total RNA was extracted from the cells and reverse-transcribed to cDNA. The presence of dsRNA in the cells was assessed by semi-quantitative PCR followed by gel electrophoresis, Figure 4 and S3.

In the absence of CPPs, naked dsRNA molecules were not efficiently internalized into the cells as indicated by the absences of dsRNA bands even after 48 h. At 1:1 P/N ratio, regardless of CPPs, the dsRNA molecules were not significantly internalized into the cells due to their negatively charged character as expected. At 50:1 P/N ratio, dsRNA molecules were internalized into the cells as early as 1 h and remained in the cells after 6 h, irrespective of CPPs used. The results suggested that both TAT and EB1 were able to carry 600-bp dsRNA molecules across the cell membrane into the cytoplasm. The initial cellular uptake appeared to be largely governed by the physical properties of nanocomplexes particularly their hydrodynamic size and cationic character which dependent on the charge ratio. These results are in agreement with previous studies reporting the cellular uptake of the cationic nanocomplexes prepared from CPPs and nucleic acids, including siRNA (Cerrato et al., 2020; Kasai et al., 2019) and plasmid DNA (Lakshmanan, Kodama, Yoshizumi, Sudesh, & Numata, 2013; Liu et al., 2016).

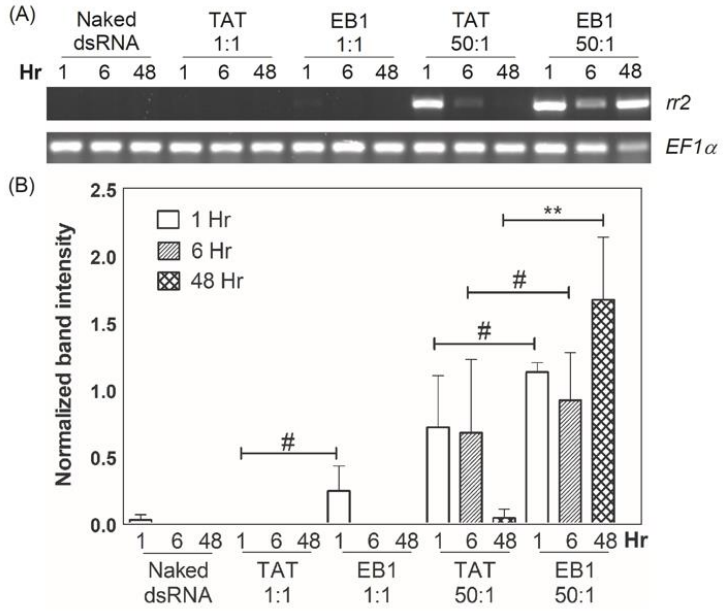

Figure 4 Cellular uptake of dsRNA after 1, 6, and 48 h. (A) Representative semi-quantitative PCR of *rr*2 and *EF-1a* genes analyzed by 1% agarose gel electrophoresis. Lane 1-3: naked dsRNA. Lane 4-6: TAT/dsRNA at a P/N ratio of 1:1. Lane 7-9: EB1/dsRNA at a P/N ratio of 1:1. Lane 10-12: TAT/dsRNA nanocomplex at a P/N ratio of 50:1. Lane 13-15: EB1/dsRNA nanocomplex at a P/N ratio of 50:1. (B) Band intensity analyzed by ImageJ program as mean ± standard deviation from three independent experiments. Statistical differences were assessed by a one-way ANOVA with Tukey's post hoc comparison; # = not significant, $^{**}p < 0.001$.

Despite no significant difference at 1 h, the dsRNA delivered into cells by EB1 remained detectable after 48 h. In contrast, the dsRNA level was diminished with TAT-mediated delivery. As the physical properties of nanocomplexes prepared from TAT and EB1 were comparable, the distinct dsRNA levels after a prolonged incubation period could be realized by two possibilities. One possibility is that the process of releasing cargoes from the endosome into the cytoplasm was different in each peptide. TAT-mediated delivery was shown to suffer from endosomal entrapment where the cargoes were trapped inside the endosomes and subsequent lysosomes. As a consequence, a certain number of cargoes was subjected to enzymatic hydrolysis preventing them from effectively functioning inside the cells (Kaplan et al., 2005; LeCher, Nowak, & McMurry, 2017; Panariti, Miserocchi, & Rivolta, 2012). EB1, modified from the penetratin peptide, is an improved CPP for endosomal escape. The sequence of EB1 contained histidine and tryptophan residues that induce endosome bursting allowing cargoes to escape from the endosome to the cytoplasm. Subsequently, the biological functions of cargoes were achieved more effectively in the cytoplasm of the cells (Lundberg et al., 2007). The detectable dsRNA level in EB1-mediated delivery observed in this study was likely because EB1 induced endosomal escape allowing dsRNA to localize in the cytoplasm while dsRNA mediated by non-endosomolytic TAT delivery was subjected to degradation process. As a result, delivered dsRNA that survive lysosomal degradation was consequently available as a template for PCR amplification.

Another possibility of distinct dsRNA levels at 48 h was that TAT and EB1 exhibited different internalization profiles. Eiríksdóttir et al. (2010) reported that TAT exhibited a fast uptake profile at the initial entry and after that, the internalization dropped rapidly in less than 30 min. On the other hand, EB1 showed a slower uptake profile with continuous delivery for 2 h. Typically, after prolonged incubation, the level of dsRNA was unlikely to be observed as the dsRNA readily undergoes the RNAi process, which degrades the delivered dsRNA along with the mRNA target. However, in our work, the mRNA target was absent in Sf9 cells. Thus, the dsRNA that was continuously delivered by EB1 remains detectable at 48 h without RNAi-mediated degradation.

In this work, we explored the possibility of using CPPs as a carrier to improve the internalization of long dsRNA in the arthropod cell line. With the optimal ratio, the cationic nanocomplexes can be formed allowing the uptake of dsRNA into the cells. Similar events have been observed for the delivery of dsRNA using other cationic nanocarriers such as liposome and polymer. These carriers can deliver long dsRNA with a size ranging from 150-400 bp into arthropod cells (Cooper et al., 2021; Lin et al., 2017; Sanitt et al., 2016; Ufaz et al., 2018). This is also observed in our work where cationic CPPs can deliver 600-bp dsRNA into Sf9 cells. In general, these carriers including CPPs protect the dsRNA from nuclease digestion and thus minimizing dsRNA degradation. The toxicity of the nanocomplexes prepared from these carriers was dependent on the cationic charge density, the concentration of nanocomplexes, and the type of the cells (El-Andaloussi, Järver, Johansson, & Langel, 2007; Fischer, Li, Ahlemeyer, Krieglstein, & Kissel, 2003; Romøren, Thu, Bols, & Evensen, 2004). Therefore, more carefully designed experiments must be performed to compare the toxicity between each system. In addition to cellular uptake efficiency and toxicity, physical properties also influence the RNAi efficacy. For example, chitosan is one of the widely used cationic polymers in agricultural applications. It has been shown to deliver siRNA and dsRNA for the protection of shrimp from viral disease and for the insect pest control via RNAi (Gurusamy et al., 2020; Theerawanitchpan et al., 2012; Ufaz et al., 2018). However, chitosan is insoluble at neutral and basic pH of which is the condition used for dissolving dsRNA. This limitation could affect the preparation reproductivity and subsequent RNAi efficacy in the cells.

A major obstacle to deliver dsRNA by these carriers is endosomal entrapment (Dhandapani et al., 2019; Kaplan et al., 2005). To overcome this issue, chemical modification of the nanocarriers was applied to induce endosomal escape. Examples include fusion of endosomal-disruptive peptides, incorporation of cholesterol into a liposome, or increase of cationic charge density on polymer (Kim et al., 2005; Pei & Buyanova, 2019; Yamada et al., 2015). Interestingly, the properties of CPPs can be tailored by simply manipulating the amino acid sequences to improve the RNAi efficacy. This opens the possibility to screen for CPPs that are suitable for

each specific application. Our work showed that CPPs are a potential candidate for the delivery of long dsRNA. Further experiments must be performed in different arthropod cells at relevant conditions to evaluate the RNAi efficacy as well as to assess the toxicity of this delivery system.

5. Conclusion

Double-stranded RNA binds non-covalently to cationic cell-penetrating peptides, TAT and EB1. At an appropriate ratio, cationic complexes with size in nanometer ranges can be formed. The internalization efficiency of nanocomplexes was governed by the physical properties such as zeta potential and size, as well as the amino acid sequences. This work provides physical character information of nanocomplexes that can be useful for developing nucleic acid delivery systems in agricultural applications.

6. Acknowledgements

This research is supported in part by the Graduate Program Scholarship from the Graduate School, Kasetsart University and Kasetsart University Research and Development Institute (KURDI) grant number VorTorDor 100.58. Authors thank Panyarat Laurchan for assistant with image analysis, Jarupund Pakawat for assistance with statistical analysis. Authors thank the Specialized center of Rubber and Polymer Materials for agriculture and industry (RPM), Faculty of Science, Kasetsart University for the support.

7. References

Al Soraj, M., He, L., Peynshaert, K., Cousaert, J., Vercauteren, D., Braeckmans, K., De Smedt, S. C., Jones, A. T. (2012). siRNA and pharmacological inhibition of endocytic pathways to characterize the differential role of macropinocytosis and the actin cytoskeleton on cellular uptake of dextran and cationic cell penetrating peptides octaarginine (R8) and HIV-Tat. *Journal of Controlled Release*, *161*(1), 132-141. DOI: https://doi.org/10.1016/j.jconrel.2012.03.015

Attasart, P., Kaewkhaw, R., Chimwai, C., Kongphom, U., Namramoon, O., & Panyim, S. (2009). Inhibition of white spot syndrome virus replication in Penaeus monodon by combined silencing of viral rr2 and shrimp PmRab7. *Virus Research*, *145*(1), 127-133. DOI: https://doi.org/10.1016/j.virusres.2009.06.018

Brutscher, L. M., & Flenniken, M. L. (2015). RNAi and antiviral defense in the honey bee. *Journal of Immunology Research*, *2015*, 941897. DOI: https://doi.org/10.1155/2015/941897

Cermenati, G., Terracciano, I., Castelli, I., Giordana, B., Rao, R., Pennacchio, F., & Casartelli, M. (2011). The CPP Tat enhances eGFP cell internalization and transepithelial transport by the larval midgut of Bombyx mori (Lepidoptera, Bombycidae). *Journal of Insect Physiology*, *57*(12), 1689-1697. DOI: https://doi.org/10.1016/j.jinsphys.2011.09.004

Cerrato, C. P., Kivijärvi, T., Tozzi, R., Lehto, T., Gestin, M., & Langel, Ü. (2020). Intracellular delivery of therapeutic antisense oligonucleotides targeting mRNA coding mitochondrial proteins by cell-penetrating peptides. *Journal of Materials Chemistry B*, *8*(47), 10825-10836. DOI: https://doi.org/10.1039/D0TB01106A

Christiaens, O., Niu, J., & Taning, C. N. T. (2020). RNAi in Insects: A Revolution in Fundamental Research and Pest Control Applications. *Insects*, *11*(7). DOI: https://doi.org/10.3390/insects11070415

Clogston, J. D., & Patri, A. K. (2011). Zeta potential measurement. *Methods Mol Biol*, *697*, 63-70. DOI: https://doi.org/10.1007/978-1-60327-198-1_6

Cooper, A. M., Song, H., Yu, Z., Biondi, M., Bai, J., Shi, X., Ren, Z., Weerasekara, S. M., Hua, D. H., Silver, K., Zhang, J., Zhu, K. Y. (2021). Comparison of strategies for enhancing RNA interference efficiency in Ostrinia nubilalis. *Pest Management Science*, *77*(2), 635-645. DOI: https://doi.org/10.1002/ps.6114

Dhandapani, R. K., Gurusamy, D., Howell, J. L., & Palli, S. R. (2019). Development of CS-TPP-dsRNA nanoparticles to enhance RNAi efficiency in the yellow fever mosquito, Aedes aegypti. *Scientific*

Reports, *9*(1), 8775. DOI: https://doi.org/10.1038/s41598-019-45019-z

Edwards, C. H., Christie, C. R., Masotti, A., Celluzzi, A., Caporali, A., & Campbell, E. M. (2020). Dendrimer-coated carbon nanotubes deliver dsRNA and increase the efficacy of gene knockdown in the red flour beetle Tribolium castaneum. *Scientific Reports*, *10*(1), 12422. DOI: https://doi.org/10.1038/s41598-020-69068-x

Eiríksdóttir, E., Mäger, I., Lehto, T., El Andaloussi, S., & Langel, U. (2010). Cellular internalization kinetics of (luciferin-)cell-penetrating peptide conjugates. *Bioconjug Chem*, *21*(9), 1662-1672. DOI: https://doi.org/10.1021/bc100174y

El-Andaloussi, S., Järver, P., Johansson, H. J., & Langel, U. (2007). Cargo-dependent cytotoxicity and delivery efficacy of cell-penetrating peptides: a comparative study. *Biochem J*, *407*(2), 285-292. DOI: https://doi.org/10.1042/bj20070507

Feinberg, E. H., & Hunter, C. P. (2003). Transport of dsRNA into cells by the transmembrane protein SID-1. *Science*, *301*(5639), 1545-1547. DOI: https://doi.org/10.1126/science.1087117

Fischer, D., Li, Y., Ahlemeyer, B., Krieglstein, J., & Kissel, T. (2003). In vitro cytotoxicity testing of polycations: influence of polymer structure on cell viability and hemolysis. *Biomaterials*, *24*(7), 1121-1131. DOI: https://doi.org/10.1016/S0142-9612(02)00445-3

Foroozandeh, P., & Aziz, A. A. (2018). Insight into Cellular Uptake and Intracellular Trafficking of Nanoparticles. *Nanoscale research letters*, *13*(1), 339-339. DOI: https://doi.org/10.1186/s11671-018-2728-6

Frankel, A. D., & Pabo, C. O. (1988). Cellular uptake of the tat protein from human immunodeficiency virus. *Cell*, *55*(6), 1189-1193. DOI: https://doi.org/10.1016/0092-8674(88)90263-2

Green, M., & Loewenstein, P. M. (1988). Autonomous functional domains of chemically synthesized human immunodeficiency virus tat trans-activator protein. *Cell*, *55*(6), 1179-1188. DOI: https://doi.org/10.1016/0092-8674(88)90262-0

Gurusamy, D., Mogilicherla, K., & Palli, S. R. (2020). Chitosan nanoparticles help double-stranded RNA escape from endosomes and improve RNA interference in the fall armyworm, Spodoptera frugiperda. *Archives of Insect Biochemistry and Physiology*, *104*(4), e21677. DOI: https://doi.org/10.1002/arch.21677

Huang, Y.-W., Lee, H.-J., Tolliver, L. M., & Aronstam, R. S. (2015). Delivery of Nucleic Acids and Nanomaterials by Cell-Penetrating Peptides: Opportunities and Challenges. *BioMed Research International*, *2015*, 834079. DOI: https://doi.org/10.1155/2015/834079

Joga, M. R., Zotti, M. J., Smagghe, G., & Christiaens, O. (2016). RNAi Efficiency, Systemic Properties, and Novel Delivery Methods for Pest Insect Control: What We Know So Far. *Frontiers in Physiology*, *7*(553). DOI: https://doi.org/10.3389/fphys.2016.00553

Kaplan, I. M., Wadia, J. S., & Dowdy, S. F. (2005). Cationic TAT peptide transduction domain enters cells by macropinocytosis. *Journal of Controlled Release*, *102*(1), 247-253. DOI: https://doi.org/10.1016/j.jconrel.2004.10.018

Kasai, H., Inoue, K., Imamura, K., Yuvienco, C., Montclare, J. K., & Yamano, S. (2019). Efficient siRNA delivery and gene silencing using a lipopolypeptide hybrid vector mediated by a caveolae-mediated and temperature-dependent endocytic pathway. *Journal of nanobiotechnology*, *17*(1), 11-11. DOI: https://doi.org/10.1186/s12951-019-0444-8

Kim, T. H., Kim, S. I., Akaike, T., & Cho, C. S. (2005). Synergistic effect of poly(ethylenimine) on the transfection efficiency of galactosylated chitosan/DNA complexes. *J Control Release*, *105*(3), 354-366. DOI: https://doi.org/10.1016/j.jconrel.2005.03.024

Laisney, J., Gurusamy, D., Baddar, Z. E., Palli, S. R., & Unrine, J. M. (2020). RNAi in *Spodoptera frugiperda* Sf9 cells via nanomaterial mediated delivery of dsRNA: A comparison of poly-l-arginine polyplexes and poly-l-arginine-functionalized Au nanoparticles. *ACS Applied Materials & Interfaces*, *12*(23), 25645-25657. DOI: https://doi.org/10.1021/acsami.0c06234

Lakshmanan, M., Kodama, Y., Yoshizumi, T., Sudesh, K., & Numata, K. (2013). Rapid and efficient gene delivery into plant cells using designed peptide carriers. *Biomacromolecules*, *14*(1), 10-16. DOI: https://doi.org/10.1021/bm301275g

LeCher, J. C., Nowak, S. J., & McMurry, J. L. (2017). Breaking in and busting out: cell-penetrating peptides and the endosomal escape problem. *Biomolecular concepts*, *8*(3-4), 131-141. DOI: https://doi.org/10.1515/bmc-2017-0023

Lin, Y.-H., Huang, J.-H., Liu, Y., Belles, X., & Lee, H.-J. (2017). Oral delivery of dsRNA lipoplexes to German cockroach protects dsRNA from degradation and induces RNAi response. *Pest Management Science*, *73*(5), 960-966. DOI: https://doi.org/10.1002/ps.4407

Liu, B. R., Huang, Y.-W., Aronstam, R. S., & Lee, H.-J. (2016). Identification of a Short Cell-Penetrating Peptide from Bovine Lactoferricin for Intracellular Delivery of DNA in Human A549 Cells. *PLOS ONE*, *11*(3), e0150439. DOI: https://doi.org/10.1371/journal.pone.0150439

Liu, C., Liu, X.-N., Wang, G.-L., Hei, Y., Meng, S., Yang, L.-F., Yuan, L., & Xie, Y. (2017). A dual-mediated liposomal drug delivery system targeting the brain: rational construction, integrity evaluation across the blood-brain barrier, and the transporting mechanism to glioma cells. *International journal of nanomedicine*, *12*, 2407-2425. DOI: https://doi.org/10.2147/IJN.S131367

Liu, W.-J., Chang, Y.-S., Wang, C.-H., Kou, G.-H., & Lo, C.-F. (2005). Microarray and RT-PCR screening for white spot syndrome virus immediate-early genes in cycloheximide-treated shrimp. *Virology*, *334*(2), 327-341. DOI: https://doi.org/10.1016/j.virol.2005.01.047

Lundberg, P., El-Andaloussi, S., Sütlü, T., Johansson, H., & Langel, Ü. (2007). Delivery of short interfering RNA using endosomolytic cell-penetrating peptides. *The FASEB Journal*, *21*(11), 2664-2671. DOI: https://doi.org/10.1096/fj.06-6502com

McEwan, D. L., Weisman, A. S., & Hunter, C. P. (2012). Uptake of extracellular double-stranded RNA by SID-2. *Molecular Cell*, *47*(5), 746-754. DOI: https://doi.org/10.1016/j.molcel.2012.07.014

Panariti, A., Miserocchi, G., & Rivolta, I. (2012). The effect of nanoparticle uptake on cellular behavior: disrupting or enabling functions? *Nanotechnology, science and applications*, *5*, 87-100. DOI: https://doi.org/10.2147/NSA.S25515

Pei, D., & Buyanova, M. (2019). Overcoming endosomal entrapment in drug delivery. *Bioconjug Chem*, *30*(2), 273-283. DOI: https://doi.org/10.1021/acs.bioconjchem.8b00778

Romøren, K., Thu, B. J., Bols, N. C., & Evensen, Ø. (2004). Transfection efficiency and cytotoxicity of cationic liposomes in salmonid cell lines of hepatocyte and macrophage origin. *Biochimica et Biophysica Acta (BBA) - Biomembranes*, *1663*(1), 127-134. DOI: https://doi.org/10.1016/j.bbamem.2004.02.007

Sanitt, P., Apiratikul, N., Niyomtham, N., Yingyongnarongkul, B. E., Assavalapsakul, W., Panyim, S., & Udomkit, A. (2016). Cholesterol-based cationic liposome increases dsRNA protection of yellow head virus infection in *Penaeus vannamei*. *Journal of Biotechnology*, *228*, 95-102. DOI: https://doi.org/10.1016/j.jbiotec.2016.04.049

Schneider, C. A., Rasband, W. S., & Eliceiri, K. W. (2012). NIH Image to ImageJ: 25 years of image analysis. *Nature methods*, *9*(7), 671-675. DOI: https://doi.org/10.1038/nmeth.2089

Shu, B., Zhang, J., Zeng, J., Cui, G., & Zhong, G. (2019). Stability of selected reference genes in Sf9 cells treated with extrinsic apoptotic agents. *Scientific Reports*, *9*(1), 14147. DOI: https://doi.org/10.1038/s41598-019-50667-2

Shukla, J. N., Kalsi, M., Sethi, A., Narva, K. E., Fishilevich, E., Singh, S., Mogilicherla, K., & Palli, S. R. (2016). Reduced stability and intracellular transport of dsRNA contribute to poor RNAi response in lepidopteran insects. *RNA biology*, *13*(7), 656-669. DOI: https://doi.org/10.1080/15476286.2016.1191728

Sifuentes-Romero, I., Milton, S. L., & García-Gasca, A. (2011). Post-transcriptional gene silencing by RNA interference in non-mammalian vertebrate systems: Where do we stand? *Mutation Research/Reviews in Mutation Research*, *728*(3), 158-171. DOI: https://doi.org/10.1016/j.mrrev.2011.09.001

Theerawanitchpan, G., Saengkrit, N., Sajomsang, W., Gonil, P., Ruktanonchai, U., Saesoo, S., Flegel, T. W., & Saksmerprome, V. (2012). Chitosan and its quaternized derivative as effective long dsRNA carriers targeting shrimp virus in Spodoptera frugiperda 9 cells. *Journal of Biotechnology*, *160*(3), 97-104. DOI: https://doi.org/10.1016/j.jbiotec.2012.04.011

Ufaz, S., Balter, A., Tzror, C., Einbender, S., Koshet, O., Shainsky-Roitman, J., Yaari, Z., & Schroeder, A. (2018). Anti-viral RNAi nanoparticles protect shrimp against white spot disease. *Molecular Systems Design & Engineering*, *3*(1), 38-48. DOI: https://doi.org/10.1039/C7ME00092H

Uhl, P., Grundmann, C., Sauter, M., Storck, P., Tursch, A., Özbek, S., Leotta, K., Roth, R., Witzigmann, D., Kulkarni, J. A., Fidelj, V., Kleist, C., Cullis, P. R., Fricker, G., & Mier, W. (2020). Coating of PLA-nanoparticles with cyclic, arginine-rich cell penetrating peptides enables oral delivery of liraglutide. *Nanomedicine: Nanotechnology, Biology and Medicine*, *24*, 102132. DOI: https://doi.org/10.1016/j.nano.2019.102132

Wei, Y., Niu, J., Huan, L., Huang, A., He, L., & Wang, G. (2015). Cell penetrating peptide can transport dsRNA into microalgae with thin cell walls. *Algal Research*, *8*, 135-139. DOI: https://doi.org/10.1016/j.algal.2015.02.002

Xie, J., Bi, Y., Zhang, H., Dong, S., Teng, L., Lee, R. J., & Yang, Z. (2020). Cell-penetrating peptides in diagnosis and treatment of human diseases: From preclinical research to clinical application. *Frontiers in pharmacology*, *11*, 697-697. DOI: https://doi.org/10.3389/fphar.2020.00697

Yamada, Y., Perez, S. M., Tabata, M., Abe, J., Yasuzaki, Y., & Harashima, H. (2015). Efficient and high-speed transduction of an antibody into living cells using a multifunctional nanocarrier system to control intracellular trafficking. *Journal of Pharmaceutical Sciences*, *104*(9), 2845-2854. DOI: https://doi.org/10.1002/jps.24310